RSC Advances

ROYAL SOCIETY OF CHEMISTRY

www.rsc.org/advances

Highly sensitive turn-on fluorescent detection of cartap via a nonconjugated gold nanoparticle-quantum dot pair mediated by inner filter effect

Jiajia Guo[a], Xin Liu[a], Hanting Gao[a], Jiaxin Bie[a], Yan Zhang[b], Baofeng Liu[c], Chunyan Sun[a, *]

[a] Department of Food Quality and Safety, Jilin University, Changchun 130062, China

[b] Laboratory of Nutrition and Functional Food, Jilin University, Changchun 130062, China

[c] National Analytical Research Center of Electrochemistry and Spectroscopy, Changchun Institute of Applied Chemistry, Chinese Academy of Sciences, Changchun 130022, China

Abstract

We describe here a simple fluorometric assay for the highly sensitive detection of cartap on the basis of the inner-filter effect (IFE) of gold nanoparticles (AuNPs) on the fluorescence of CdTe quantum dots (QDs). In the presence of AuNPs, the fluorescence of CdTe QDs was significantly quenched due to the intensive absorption of AuNPs at the 522 nm plasmon band. The well-dispersed AuNPs exhibited a tendency to aggregate when exposed to cartap with the positively charged amine groups, which induced the absorption band transition from 522 nm to the long-wavelength band and restored the IFE-decreased emission of CdTe QDs for cartap detection. Under the optimum conditions, the response was linearly proportional to the concentration of cartap in Chinese cabbage within the range of 0.01~0.50 mg/kg with a detection limit of 8.24 μg/kg (*S/N*=3). Further application in cartap-spiked vegetable samples suggested a recovery between 81.9% and 90.6%. The

*Corresponding authors. Tel.:+86 431 87836375; fax: +86 431 87836391 (C. Sun).
E-mail addresses: sunchuny@jlu.edu.cn; sunchunyan1977@163.com (C. Sun).

cartap account in the spiked samples detected by the present method and GC-MS is in good accordance, which indicates that this IFE-based fluorescent method is reliable and practical. The proposed assay exhibited good reproducibility and accuracy, providing a simple and rapid method for the analysis of cartap.

Keywords: Inner filter effect; CdTe quantum dots; Au nanoparticles; Cartap; Fluorescence quenching

Introduction

Cartap is a widely used insecticide which belongs to a member of nereistoxin derivatives and acts on nicotinic acetylcholine receptor site. Due to its low toxicity and high insecticidal activity, it is one of the most widely utilized pesticides in agriculture for crop protection and garden markets.[1-3] However, the overuse of cartap could lead to dangerous levels of residues, which enters the food supply chain and results in an unexpected hazard for human health. The presence of cartap residues in fruit and vegetable crops as well as in water has been shown to inhibit lysyl oxidase activity and cause significant neuromuscular toxicity, resulting in respiratory failure.[4,5] Therefore, maximum residue limits (MRLs) for cartap have been defined by food administrations. For example, the European Commission stipulated a permissible residue limit of cartap at 0.1 mg/kg in tea,[6] and China set the maximum residue limit of cartap at 3 mg/kg in Chinese cabbage.[7]

Considering the extensive application and toxic effects of cartap, the development of a fast, simple, and highly sensitive method for the determination of cartap is highly desirable. Gas chromatography–mass spectrometry (GC–MS)[8] and

liquid chromatography–mass spectrometry (LC–MS)[9] have been established for the determination of cartap. Although these methods can offer sensitive and accurate detection results, they are complicated, time-consuming, require bulky instrumentation and have to be performed by highly trained technicians. Moreover, they are not cost-effective. Therefore, it is of considerable significance to develop sensitive, simple, and low-cost methods for the detection of cartap. Recently, a simple colorimetric method for the detection of cartap residue in agricultural products has been developed by the direct use of unmodified AuNPs as colorimetric probe.[2] Based on luminescence quenching through cartap-induced aggregation of upconversion nanocrystal/Au nanoparticle nanocomposite, a novel luminescence resonance energy transfer nanosensor has been established for cartap screening.[3] Fluorescent assays have the advantages of high sensitivity, specificity, and real-time monitoring with fast response time. Therefore, we report here a novel strategy for cartap analysis based on the inner filter effect (IFE) of fluorescence.

The inner filter effect (IFE) of fluorescence refers to the absorption of light at the excitation and/or emission wavelengths by absorbers in the detection system.[10] Although the IFE is usually considered as an annoying source of error in spectrofluorometry and should be avoided, recent studies have demonstrated that the IFE of fluorescence has emerged as an efficient strategy for the design and development of novel assays for various analytes by choosing suitable absorber-fluorophore pairs.[11-19] Different with the fluorescence resonance energy transfer (FRET), the IFE-based assays do not require the establishing of any covalent

linking between the absorber and the fluorophore, simplifying the synthesis of the fluorescent materials.[18] Since the changes on the absorbance of the absorber are translated into exponential changes on the fluorescence of the fluorophore, an enhanced sensitivity for the IFE-based assay is reasonable with respect to the absorbance alone.[19] However, IFE would occur effectively only when the absorption band of the absorber possesses a complementary overlap with the excitation and/or emission bands of the fluorophore to some extent. Therefore, restrictions generally exist in the design of IFE-based fluorescent assays such as the limited choice of suitable absorber and fluorophore with a good spectral overlap, small extinction coefficient of the conventional absorber, and so on. Au nanoparticles (AuNPs) have tremendously larger extinction coefficient (in the order of 10^8 M^{-1} cm^{-1} or more) than conventional chromophores, which enables AuNPs to be extraordinarily effective absorbers in the IFE-based fluorescence assays.[11-14,16] On the other hand, quantum dots (QDs) can function as potentially ideal fluorophores in the IFE-based fluorescent assay due to their superior luminescent properties, including high quantum yield of fluorescence, narrow/symmetric and tunable emission with broad excitation spectrum, high photobleaching threshold and excellent photostability.[11-15] In particular, the emission wavelengths of QDs can be tuned by size, compositions, and shape, which results in high flexibility in the selection of emission wavelength as well as regulation of maximum overlap with the absorption band of the absorbent dye.[14]

In this work, we present a novel fluorometric assay for the detection of cartap on the basis of the IFE of citrate-stabilized AuNPs on the fluorescence of water-soluble

CdTe QDs capped with thioglycolic acid (TGA). This approach does not require the chemical linkage between AuNPs and QDs, which offers considerable flexibility and more simplicity in probe fabrication and experimental design. The principle of this method is illustrated in Scheme 1. The citrate-stabilized AuNPs were claret-red and well-dispersed with the strong characteristic Plasmon absorption at 522 nm (1). Thus, because of the large overlap between the absorption of AuNPs and the emission of CdTe QDs, the fluorescence of CdTe QDs was obviously quenched via IFE upon addition of AuNPs (2). In the presence of cartap, the positively charged amine groups of cartap show strong interaction with AuNPs, which decreased the stability of citrate-stabilized AuNPs, rapidly inducing the aggregation of AuNPs and thereby the obvious color changes.[2] The absorption of AuNPs at 522 nm was decreased due to the cartap-induced aggregation (3). As a result, the fluorescence emission of CdTe QDs was restored properly (4), based on which cartap could be detected in a simple and sensitive approach.

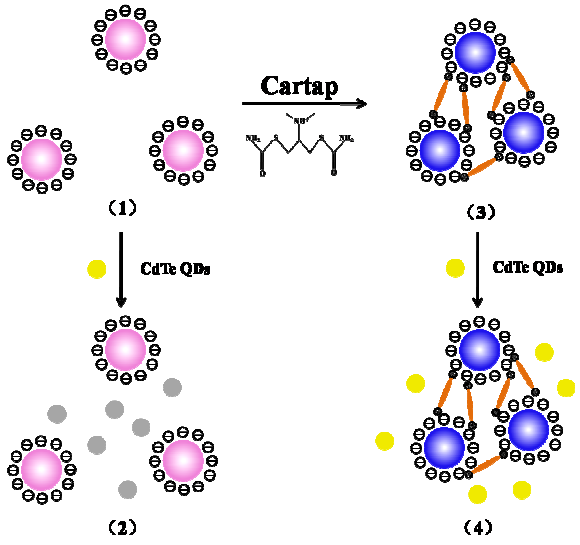

Scheme 1. Schematic illustration of rapid analysis of cartap based on the inner filter effect of AuNPs on the fluorescence of CdTe QDs.

Experimental section

Reagents and materials

Te powder, sodium borohydride ($NaBH_4$) and thioglycolic acid (TGA) were obtained from Sinopharm Chemical Reagent (Shanghai, China). Cadmium chloride ($CdCl_2 \cdot 2H_2O$), $AuCl_3 \cdot HCl \cdot 4H_2O$, sodium citrate, vitamin C, $FeCl_3$, Na_3PO_4, NaCl, $MgCl_2$, $CaCl_2$ and KCl were purchased from Beijing Chemical Reagent Company (Beijing, China). N-hexane (HPLC grade) was purchased from Fisher Scientific (USA). Cartap was purchased from Sigma-Aldrich (St. Louis, USA). If not specifically stated, all the chemicals were of analytical grade and triply distilled water was used in all experiments. Organic vegetable free from pesticides was purchased from the local supermarket.

Apparatus

A WVFY-201 microwave reactor of 800 W power (Zhize Equipment Factory, Shanghai, China) was used in the experiments. All pH measurements were carried out with a Model pHS-3C (Chenhua Equipment Factory, Shanghai, China). The ultrasonic treatment was carried out on a 125 KQ-300DE ultrasonicator (Kunshan Ultrasonic Instrument Co., Shanghai, China). UV-vis absorption spectra were recorded with a 2550 UV-vis spectrophotometer (Shimadzu, Tokyo, Japan). The fluorescence spectra were acquired on a RF-5301 fluorescence spectrophotometer (Shimadzu, Tokyo, Japan) at the excitation wavelength of 400 nm, with both of the exciting and emission slits set at 5 nm. The fluorescence lifetime measurements were conducted using a FLS 920 spectrometer (Edinburgh Instruments, UK). Zeta potential and dynamic light

scattering (DLS) were performed with a Malvern Nano-ZS apparatus for characterization of the surface charge and size distribution of nanoparticles in solution. Transmission electron microscopy (TEM) measurements were made on a TECNAI F20 (FEI Co., Holland) operated at an accelerating voltage of 200 kV. The samples for TEM characterization were prepared by placing a drop of colloidal solution on carbon-coated copper grid and dried at room temperature. Mass spectrometric analysis of cartap was performed using a 5975-6890N GC-MS system (Agilent, USA) equipped with a HP-35 column, a quaternary pumping system and an auto injector.

Preparation of citrate-stabilized AuNPs

The solution of citrate-stabilized AuNPs was synthesized according to the procedure described previously with some slight modification[20] and stored at 4 ˚C. All glassware used in these preparations was thoroughly cleaned in aqua regia, rinsed with triply distilled water, and oven-dried prior to use. In a 250 mL round-bottom flask equipped with a condenser, 4.12 mL of 1% $HAuCl_4$ was diluted to 100 mL and heated to a rolling boil with vigorous stirring. Rapid addition of 10 mL of 38.8 mM sodium citrate to the vortex of the solution resulted in a color change from pale yellow to claret-red. Boiling was continued for 10 min; the heating mantle was then removed, and stirring was continued for an additional 15 min. After the solution cooled down to room temperature, it was filtered through a 0.4 μm Millipore membrane filter. The molar extinction coefficient at ~520 nm for spherical AuNPs is 2.7×10^8 $M^{-1}\cdot cm^{-1}$,[14] thus the molar concentration of AuNPs was calculated to be approximately 1.15×10^{-8} $mol\cdot L^{-1}$ according to the Lambert Beer's law.

Preparation of water-soluble TGA-CdTe QDs

TGA-capped CdTe QDs were synthesized according to the procedure described previously with some slight modification.[21] Briefly, 0.0256 g Te powder and 0.0386 g $NaBH_4$ was firstly added into 1 mL water in a three-neck flask with a condenser attached, and reacted at 50 ˚C for 45 min to get Te precursor (NaHTe). Cd precursor was prepared by mixing a solution of $CdCl_2$ (0.09134 g) with 66 μL TGA, and the solution was diluted to 100 mL, which was then adjusted to pH 11 by 1 M NaOH and deaerated with N_2 for 20 min. The Cd precursor was added into NaHTe solution while stirring vigorously at room temperature. The molar ratio of Cd^{2+}:Te^{2-}:TGA is 1:0.5:2.4. Under the protection of N_2 atmosphere, the mixed solution was stirred for 10 min and then heated with microwaves at 50% output power for 45 min. The particle size *D* of the as-prepared CdTe QDs was calculated to be 2.73 nm according to the excitonic absorption peak value and the concentration of QDs is approximately 1.12×10^{-5} $mol\cdot L^{-1}$ based on the molar extinction coefficient (ε=10,043 $(D)^{2.12}$) of CdTe nanoparticles.[22]

General procedures for IFE-based fluorescence detection of cartap

A typical IFE-based analysis for cartap was performed as follows. 0.5 mL of AuNPs solution and 1.4 mL buffer (pH=7.0, HCl/NaOH) were added into 4 mL centrifuge tubes with 0.5 mL of cartap solution with different concentrations, and the mixture was incubated at room temperature for 10 min. Then, 0.6 mL of CdTe QDs (2.25×10^{-6} $mol\cdot L^{-1}$) was added into the above prepared solution. Afterwards, the fluorescence emission spectra were recorded with the excitation of 400 nm. The

calibration curve for cartap was established according to the fluorescence enhancement efficiency, which was monitored by $(F\text{-}F_0)/F_0$ where F_0 and F are the maximum emission intensity of the system in the absence and presence of cartap, respectively.

Procedures for cartap detection in Chinese cabbage

Cartap in Chinese cabbage was measured to evaluate the potential of this assay for insecticides screening in real-world applications. Chinese cabbage samples were pretreated according to the method of GB/T 5009.199.2003.[23] 2 g of Chinese cabbage was weighed and finely chopped to 1 cm^3, then dissolved in 5 mL purified water and ultrasonicated for 2 min. After standing for 3-5 min, different concentrations of cartap standard solutions were added into the obtained matrix of Chinese cabbage samples. The supernatant was collected for analysis according to the general procedures for IFE-based fluorescence detection of cartap. For recoveries experiment, known quantities of cartap were injected into the finely-chopped Chinese cabbage, then pretreated and analyzed according to the above procedures.

Procedures for cartap detection in Chinese cabbage by GC-MS

To measure cartap by GC-MS method, Chinese cabbage was pretreated by a method of multiple liquid–liquid extractions with alterations.[2,24] Typically, 2 g of Chinese cabbage and 40 mL of 0.05 M HCl were ultrasonicated for 20 min at 80 ˚C. The mixture was centrifuged at 4000 rpm for 5 min. The resulted supernatant was washed with 30 mL of n-hexane and 0.1 g activated carbon, and then centrifuged at 4000 rpm for 5 min after vortex for 1 min. The upper layer was discarded, and the

lower layer was washed with another 30 mL of n-hexane again. After that, the aqueous layer was carefully adjusted to pH 8.5–9.0 with 2 M NaOH. Finally, 5 mL of 50 g/L $NaHCO_3$ and 4 mL of n-hexane were added to the organic layer. The mixture was shaken for 1 min and centrifuged at 4000 rpm for 5 min. The organic layer was collected for determination.

The GC–MS was equipped with a fused-silica capillary column (30 m×0.25 mm×0.25 μm). The column temperature was start at 100 °C, held 2 min, then programmed to heat from 100 to 240 °C at 15 °C/min, and held 5 min. The temperature of the injection port was set at 280 °C. Splitless injection mode was used. The carrier gas was helium, and its flow rate was set at 1 mL/min. The MS was operated in the electron impact (EI) mode using 70 eV ionization. The ion source tempertature was 230 °C.

Results and discussion

IFE of AuNPs on the fluorescence of CdTe QDs

Fig. 1 shows the absorption spectrum of AuNPs (curve a) and the fluorescence emission spectrum of CdTe QDs (curve b). The claret-red aqueous solution of AuNPs displays intense characteristic surface Plasmon absorption at 522 nm, demonstrating that the obtained AuNPs was well-dispersed. The average diameter of the as-prepared AuNPs was observed about 18 nm according to the TEM and DLS measurements. The water-soluble TGA-capped CdTe QDs were prepared through a microwave-assisted aqueous-phase synthesis, and they show a fluorescence emission maximum at 540 nm, which was near the absorption maximum of AuNPs. It can also

be seen that the fluorescence spectrum band is narrow and symmetric (the width at half-maximum is about 56 nm), indicating that the QDs are monodisperse and uniform. The average particle size of as-prepared QDs is about 2.73 nm, derived from the wavelength of the first excitonic absorption peak (λ_{max}=516 nm) based on the emipirical fitting function from the previous report.[22] The DLS measurement also demonstrated the size distribution of CdTe QDs with the main particle diameter of 2.81 nm, which is consistent with the calculation result. It is obvious that the emission spectrum of CdTe QDs overlaps well with the absorption spectrum of AuNPs. Thus, the effective emission intensity of CdTe QDs might be greatly decreased or even entirely quenched due to the IFE of AuNPs if the two materials coexist.

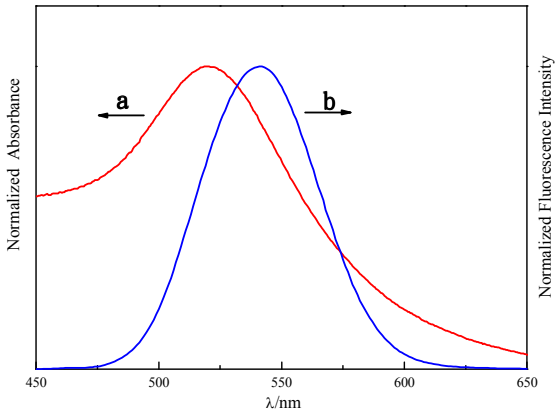

Fig. 1. Absorption spectrum of AuNPs (a) and fluorescence emission spectrum of CdTe QDs (b).

To verify the possible existence of IFE between AuPs and CdTe QDs, we mixed CdTe QDs with different concentrations of AuNPs and monitored the fluorescence changes of CdTe QDs. As shown in Fig. 2A, the emission intensity of CdTe QDs decreased gradually upon increasing the concentration of AuNPs. The citrate-stabilized AuNPs in aqueous solution are stabilized against aggregation due to

the negative capping agent's (citrate ion) electrostatic repulsion against van der Waals attraction between AuNPs. So, the well-dispersed AuNPs possess negative charge, which was confirmed by the zeta potential of -39.5 mV. The zeta potential of TGA-capped CdTe QDs was measured to be -28.6 mV, due to the ionization of the –COOH group in TGA (pKa=3.53).[25] Thus, there is no electrostatic attractive interaction between the negatively charged AuNPs and the negatively charged CdTe QDs. Furthermore, no complex formation was expected between them, which was supported by the fact that the absorption spectrum of AuNPs remained unchanged in the presence of CdTe QDs (Fig. 2B). Fluorescence lifetime measurements can provide further support for IFE-based fluorescence decrease of CdTe QDs induced by AuNPs. As expected (Fig. 3), the average lifetime of negatively charged TGA-CdTe QDs was hardly changed in the presence of negatively charged citrate-stabilized AuNPs. Therefore, the observed fluorescence decrease was not a result of the FRET process between CdTe QDs and AuNPs but should be attributed to the IFE of AuNPs on the fluorescence of CdTe QDs. With the increment of the concentration of AuNPs, the absorbance of the absorber increased, which accordingly diminished the emission light from CdTe QDs. Notably, due to the high extinction coefficient of AuNPs, the fluorescence intensity of 4.5×10^{-7} mol L^{-1} CdTe QDs decreased by over 75% in the presence of 1.92×10^{-9} mol·L^{-1} AuNPs. Hence, the fluorescence emission of CdTe QDs at 540 nm could be modulated by the absorbance of AuNPs via IFE in a sensitive and simple approach.

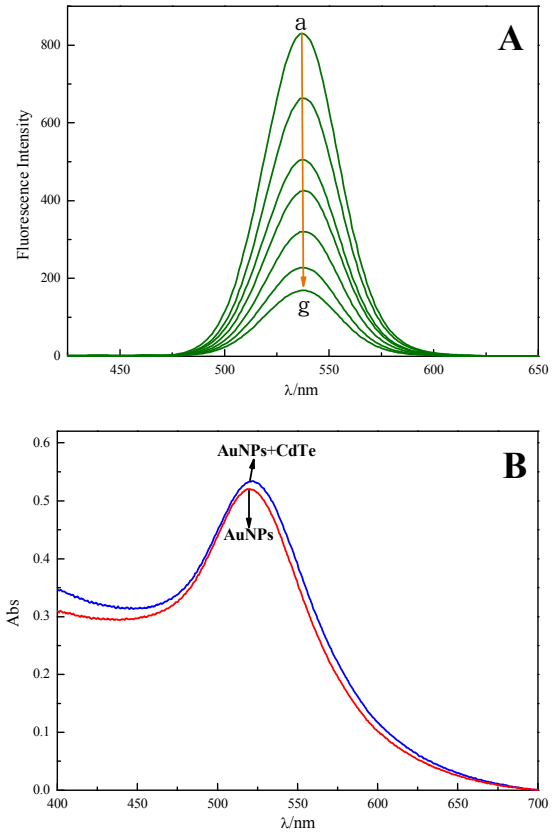

Fig. 2. (A) Fluorescence emission spectra of CdTe QDs (4.5×10^{-7} mol·L^{-1}) in the presence of increasing concentrations of AuNPs (a-g: 0, 3.2×10^{-10}, 6.4×10^{-10}, 9.6×10^{-10}, 1.28×10^{-9}, 1.6×10^{-9}, 1.92×10^{-9} mol·L^{-1}). (B) Absorption spectra of AuNPs (1.92×10^{-9} mol·L^{-1}) with and without CdTe QDs (4.5×10^{-7} mol·L^{-1}).

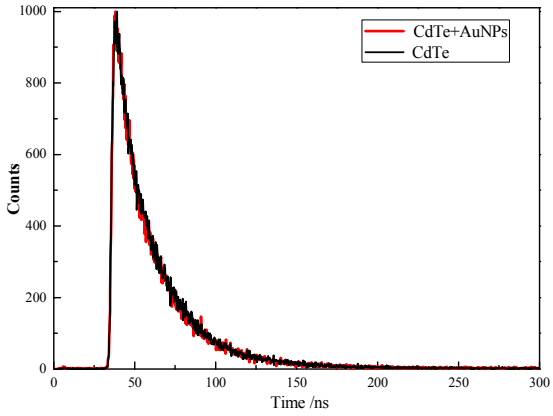

Fig. 3. Effects of AuNPs on the fluorescence lifetime of CdTe QDs. CdTe QDs (τ=23.5 ns); CdTe QDs in the presence of AuNPs (τ=22.5 ns).

Absorption changes of AuNPs in the presence of cartap

The AuNPs solution appeared red in color and exhibited an absorption peak at 522 nm. Fig. 4A presents the absorption spectrum of AuNPs in the presence of cartap with different concentrations. It is obviously seen that cartap can induce the absorbance decrease of AuNPs at 522 nm and the appearance of a small absorption peak at the longer wavelengh. As shown in Scheme 1, positively charged cartap is inclined to adsorb onto the surface of negatively charged AuNPs by electrostatic interactions, resulting in the aggregation of AuNPs accompanied with the red-to-purple (or blue) color change within several minutes. In order to know the microstructure and size distribution of the AuNPs without and with cartap, the TEM images and DLS spectra (Fig. 4B and C) were obtained. Note that in the absence of cartap, the AuNPs are mono-dispersed, whereas the AuNPs aggregate together in the presence of cartap. The results were consistent with the changes of the UV-vis absorption spectra.

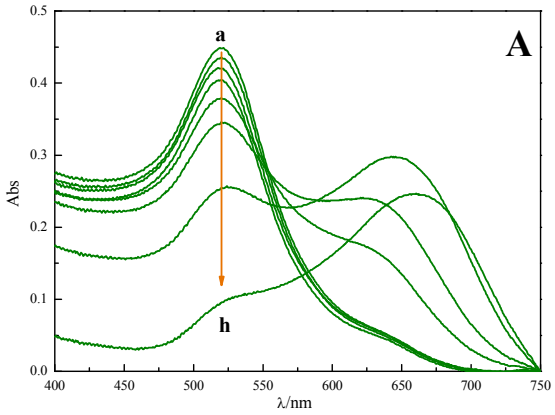

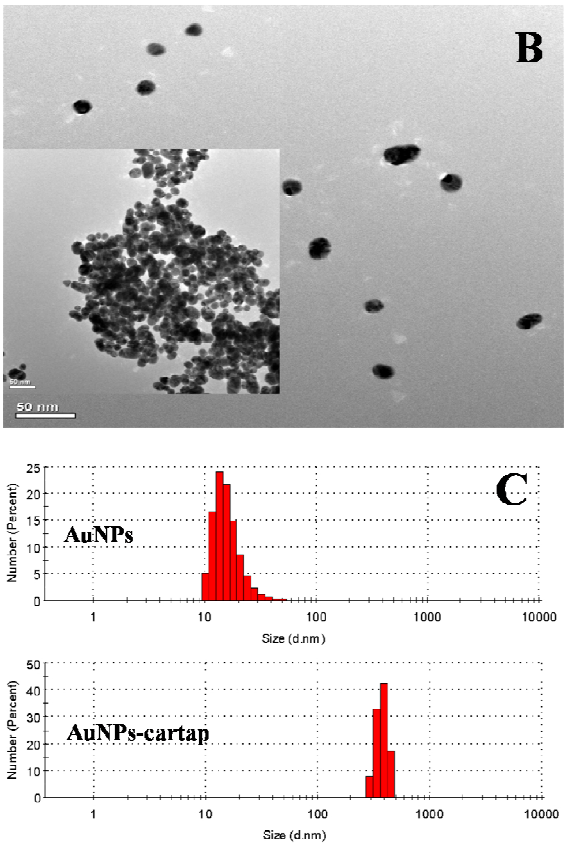

Fig. 4. (A) Absorption spectra of AuNPs (1.92×10^{-9} mol·L^{-1}) in the presence of cartap at various concentrations. The cartap in samples (a)–(h) is 0, 0.1, 0.5, 0.7, 1, 1.2, 1.5, 2 μg·mL^{-1} respectively; (B) TEM image of AuNPs, and the inset is TEM image of AuNPs after addition of cartap. (C) DLS images of AuNPs and AuNPs after addition of cartap.

Fluorescence detection of cartap through the IFE of AuNPs on the fluorescence of CdTe QDs

We designed a fluorescent assay based on the cartap-induced decrease of the absorbance of the absorber (AuNPs), which then recovered the IFE-decreased fluorescence of the fluorophore (CdTe QDs). As shown in Fig. 5, the absorption and fluorescence spectra of CdTe QDs (curves a in Fig. 5) were identical to those of the mixture of CdTe QDs and cartap (curves b in Fig. 5), which indicated that there was no interaction between cartap and CdTe QDs. The Plasmon absorption band of

AuNPs didn't change in the presence of CdTe QDs (curves c and d in Fig. 5A), demonstrating that there was no interaction between CdTe QDs and AuNPs. Therefore, the cartap-induced changes of absorption spectrum of AuNPs were identical with or without the presence of CdTe QDs (curves e and f in Fig. 5A), which indicated that AuNPs came into aggregation driven by cartap. When CdTe QDs was mixed with AuNPs, the fluorescence was significantly quenched (curve c in Fig. 5B) due to the IFE of AuNPs. However, the IFE-decreased fluorescence of QDs was recovered obviously with the presence of cartap (curve d in Fig. 5B). Meanwhile, no discernible change in the shape of the emission spectra of QDs is observed in the presence of cartap and AuNPs, indicating that the increased emission came from the CdTe QDs rather than any other newly formed emission centers. Considering the turn-on response of cartap to the fluorescence of CdTe QDs quenched by AuNPs, the possibility of developing a new, sensitive IFE-based fluorescent method for rapid determination of cartap was then evaluated.

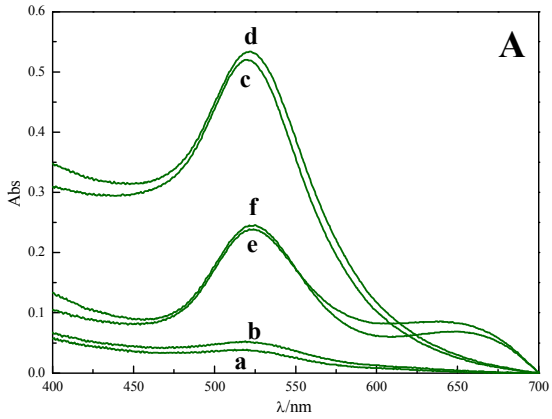

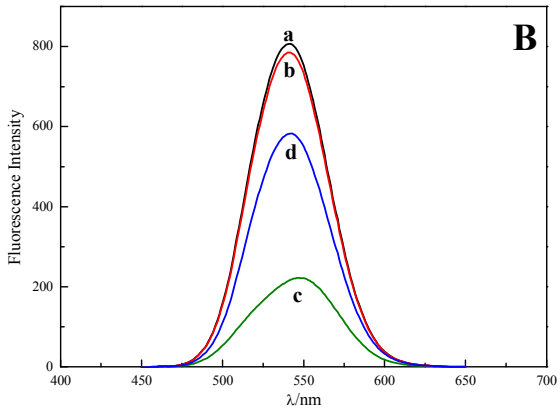

Fig. 5. (A) Absorption spectra: (a) CdTe QDs; (b) CdTe QDs and cartap; (c) AuNPs; (d) AuNPs and CdTe QDs; (e) AuNPs and cartap; (f) mixture of AuNPs, cartap and CdTe QDs. (B) Fluorescence spectra: (a) CdTe QDs; (b) CdTe QDs and cartap; (c) CdTe QDs and AuNPs; (d) mixture of AuNPs, cartap and CdTe QDs. CdTe QDs, 4.5×10^{-7} mol·L^{-1}; cartap, 1.5 μg·mL^{-1} (A) and 0.08 μg·mL^{-1} (B); AuNPs, 1.92×10^{-9} mol·L^{-1}.

The electrostatic interaction between AuNPs and cartap is intensively pH-dependent. Experimental results demonstrate that cartap could induce absorption decrease of AuNPs to a great extent at pH 7.0. On the other hand, the effects on the optical signals of the QDs-AuNPs pair are smallest at pH 7.0. Therefore, the optimal pH was chosen to be 7.0 for further experiments. The incubation time of AuNPs and cartap was optimized by recording the absorption spectrum of AuNPs every 2 min after mixing with cartap. The aggregation and spectral variation of AuNPs could be completed within 10 min. Therefore, the incubation time of AuNPs and cartap was chosen as 10 min.

IFE-based fluorescent sensing of cartap in spiked vegetable samples

Interference studies were done in order to explore the specific detection of cartap in vegetables using the IFE assay. These experiments included investigation of most commonly found substances in real samples of Chinese cabbage, such as vitamin C,

326 Fe^{3+}, Na^{+}, Mg^{2+}, K^{+}, Ca^{2+}, PO_4^{3-}. As shown in Fig. 6A, no obvious interferences were
327 noticed with the presence of these selected ions and compounds for determination of
328 cartap (i.e., the relative error in all the cases was less than 5%). Therefore, the results
329 showed no interferences from these substances in concentration levels usually found
330 in Chinese cabbage. In addition, five kinds of compounds, including methamidophos,
331 imidacloprid, methomyl, carbaryl and acetamiprid, which are common insecticides
332 used in agriculture, are detected by the present method to demonstrate its selectivity.
333 As shown in Fig. 6B, these insecticides could not disturb the selective detection of
334 cartap in the present method. Moreover, methamidophos and methomyl have thioether
335 groups similar to cartap, so we considered that there is no or negligible interaction of
336 the thioether groups with AuNPs. Thus the interaction principle between cartap and
337 AuNPs is electrostatic attraction rather than from thioether groups.

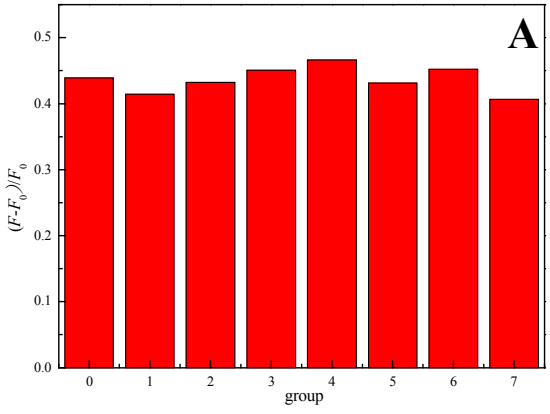

338

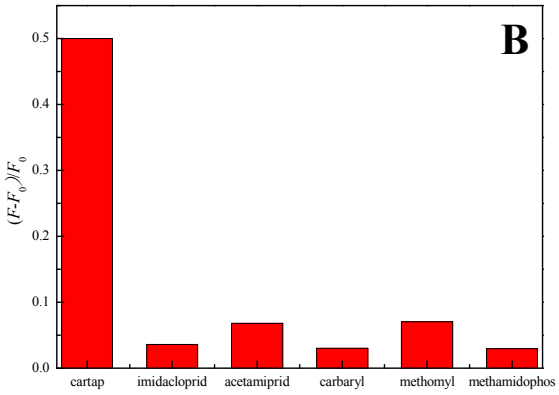

339

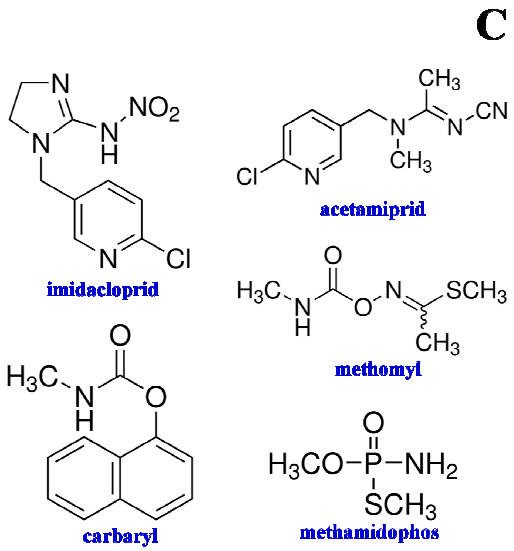

340

341 **Fig. 6.** (A) Fluorescence enhancement efficiency of CdTe QDs in the presence of 0.08 μg·mL^{-1}
342 cartap premixed with different substances. Substances: 0 control (CdTe-AuNPs-cartap); 1 vitamin
343 c (0. 45 mg·mL^{-1}); 2 Ca^{2+} (1.05 mg·mL^{-1}); 3 Fe^{3+} (8 μg·mL^{-1}); 4 K^{+} (1.07 mg·mL^{-1}); 5 Mg^{2+} (0.19
344 mg·mL^{-1}); 6 PO_4^{3-} (0.11 mg·mL^{-1}); 7 Na^{+} (0.65 mg·mL^{-1}). (B) Fluorescence enhancement
345 efficiency of CdTe QDs with different analytes. The concentrations of all insecticides are 0.08
346 μg·mL^{-1}. (C) The molecular structure of imidacloprid, acetamiprid, carbaryl, methomyl and
347 methamidophos.

348 In order to evaluate the proposed method in real samples, we studied the
349 potential applicability of this assay for detection of cartap in Chinese cabbage, and the
350 obtained results were compared with the GC-MS method. The results from GC-MS
351 demonstrate that the organic vegetable samples do not contain detectable amount of

cartap. Different concentrations of cartap standard solutions were added into the matrix of Chinese cabbage samples, and analyzed according to the IFE-based fluorescence method. Fig. 7A shows the fluorescence spectral changes of the solutions in the absence and presence of different concentrations of cartap. And the $(F\text{-}F_0)/F_0$ signal of the assay exhibited a linear correlation to concentrations of cartap spiked in Chinese cabbage (0, 0.01, 0.05, 0.10, 0.15, 0.25, 0.50 mg/kg) as displayed in the inset of Fig. 7A. The detection limit (3σ) was found to be 8.24 μg/kg, which is well below the safety limit. The relative standard deviation (RSD) was 4.6 % for the determination of 0.25 mg/kg (n=9). Fig. 7B shows the absorption spectra of AuNPs in the presence of cartap with same concentrations as Fig. 7A. Within this range of concentration, cartap could induce tiny changes on the absorption spectrum of AuNPs. Furthermore, Fig. 7C shows the quantitative relationship between AuNPs absorbance, CdTe QDs fluorescence, and cartap concentration, which indicates that tiny absorbance changes of AuNPs can cause very large fluorescence changes of CdTe QDs in the IFE-based assay. Obviously, the fluorescence method for the analysis of target objects generally display higher sensitivity than colorimetric assay. The proposed method and GC-MS method were applied to analyze cartap in the spiked samples of Chinese cabbage and the recovery results are listed in Table 1, which indicate that the proposed IFE-based fluorescence sensing is highly reproducible and accurate for rapid screening of cartap in vegetables in a simple manner.

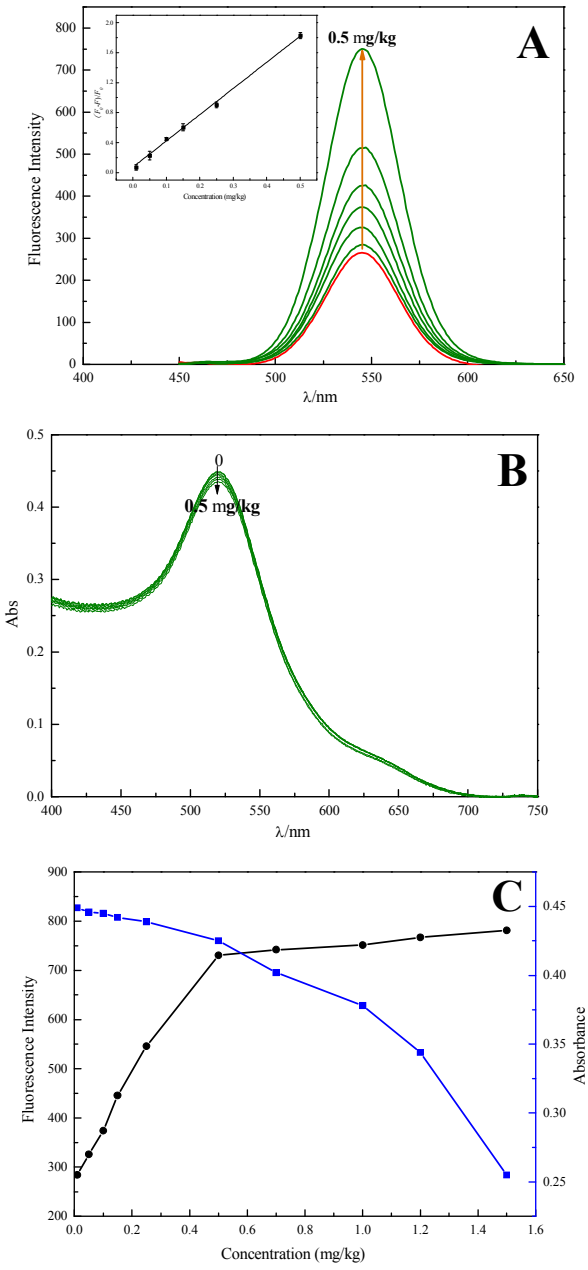

Fig. 7. (A) Fluorescence emission spectra of AuNPs-CdTe QDs in the presence of increasing concentrations of cartap in Chinese cabbage matrix (0, 0.01, 0.05, 0.10, 0.15, 0.25, 0.50 mg/kg). Inset: The linear calibration of the fluorescence enhancement efficiency versus cartap concentration. (B) Absorption spectra of AuNPs in the presence of cartap at various concentrations in Chinese cabbage matrix (0, 0.01, 0.05, 0.10, 0.15, 0.25, 0.50 mg/kg). (C) The quantitative relationship between AuNPs absorbance, CdTe QDs fluorescence, and cartap concentration in Chinese cabbage matrix (0, 0.01, 0.05, 0.10, 0.15, 0.25, 0.50, 0.70, 1.0, 1.2, 1.5 mg/kg).

Table 1 Detection of trace cartap in Chinese cabbage samples via the proposed method and GC-MS method

Sample	Amount added (mg/kg)	The proposed method		GC-MS method	
		Amount found (mg/kg)	Recovery±RSD（%）(*n*=3)	Amount found (mg/kg)	Recovery±RSD（%）(*n*=3)
Chinese cabbage	0.10	0.082	81.9±3.41	0.079	79.0±5.26
	0.25	0.217	86.8±2.18	0.186	74.4±3.87
	0.50	0.453	90.6±6.03	0.401	80.2±1.51

Conclusions

In this study, a novel sensitive and rapid fluorescent assay was developed for detection of cartap residues based on the inner filter effect (IFE) of AuNPs on CdTe QDs. The IFE efficiency of AuNPs on CdTe QDs varied with the absorption of AuNPs. In the presence of cartap, positively charged cartap could rapidly induce the aggregation of AuNPs through electrostatic interaction, and decrease their characteristic surface Plasmon absorption at 522 nm, thus attenuating the IFE efficiency between AuNPs and CdTe QDs. Thanks to the extremely high extinction coefficient of AuNPs, the strong fluorescence of CdTe QDs, and the considerable flexibility and simplicity in the experimental design, this method is easy to operate with remarkably high sensitivity for cartap detection. Under the optimum conditions, the response was linearly proportional to the concentration of cartap in Chinese cabbage within the range of 0.01-0.50 mg/kg, and the detection limit was found to be 8.24 μg/kg, which could satisfy the needs for on-site rapid monitoring of trace cartap. Moreover, this IFE-based fluorescent method was applied to analyze cartap in the spiked samples of Chinese cabbage and the recovery results were consistent with those obtained from GC-MS. Therefore, it appears to be a promising selection for

rapid screening of cartap residues in agricultural products such as vegetables.

Acknowledgments

This work was financially supported by the National Natural Science Foundation of China (No. 20905031), the Natural Science Foundation of Jilin Province (No. 201215024) and Innovation Projects of Science Frontiers and Interdisciplinary of Jilin University.

References

1. S. L. Zhou, Q. X. Dong, S. N. Li, J. F. Guo, X. X. Wang, G. N. Zhu, *Aquat. Toxicol.,* 2009, **95**, 339-346.

2. W. Liu, D. H. Zhang, Y. F. Tang, Y. H. Wang, F. Yan, Z. H. Li, J. L. Wang, H. S. Zhou, *Talanta*, 2012, **101**, 382-387.

3. Z. J. Wang, L. N. Wu, B. Z. Shen, Z. H. Jiang, *Talanta*, 2013, **114**, 124-130.

4. J. W. Liao, J. J. Kang, C. R. Jeng, S. K. Chang, M. J. Kuo, S. C. Wang, M. R. S. Liu, V. F. Pang, *Toxicol.*, 2006, **219**, 73-84.

5. H. I. Kwak, M. O. Bae, M. H. Lee, H. J. Sung, J. S. Shin, G. H. Ahn, Y. H. Kim, C. Y. Lee, M. H. Cho, *Bull. Environ. Contam. Toxicol.*, 2000, **65**, 717-724.

6.EUR-Lex,http://eur-lex.europa.eu/LexUriServ/LexUriServ.do?uri=CELEX:32000L0024:EN:HTML (accessed October 2013).

7. Chinese National Standards GB 2763-2012, Standards Press of China, Beijing, 2012.

8. A. Namera, T. Watanabe, M. Yashiki, T. Kojima, T. Urabe, *J. Chromatogr. Sci.*, 1999, **37**, 77-82.

9. I. Ferrer, E. M. Thurman, *J. Chromatogr. A*, 2007, **1175**, 24-37.

10. P. Yuan, D. R. Walt, *Anal. Chem.*, 1987, **59**, 2391-2394.

11. J. W. Li, X. M. Li, X. J. Shi, X. W. He, W. Wei, N. Ma, H. Chen, *ACS Appl. Mater. Interfaces*, 2013, **5**, 9798-9802.

12. X. Cui, M. Liu, B. X. Li, *Analyst*, 2012, **137**, 3293-3299.

13. X. Y. Cao, F. Shen, M. W. Zhang, J. J. Guo, Y. L. Luo, X. Li, H. Liu, C. Y. Sun, J. B. Liu, *Food Control*, 2013, **34**, 221-229.

14. L. Xu, B. X. Li, Y. Jin, *Talanta*, 2011, **84**, 558-564.

15. Q. Zhang, Y. Y. Qu, M. Liu, X. L. Li, J. T. Zhou, X. W. Zhang, H. Zhou, *Sens Actuators, B*, 2012, **173**, 477-482.

16. L. Shang, S. J. Dong, *Anal. Chem.*, 2009, **81**, 1465-1470.

17. L. Shang, C. J. Qin, L. H. Jin, L. X. Wang, S. J. Dong, *Analyst*, 2009, **134**, 1477-1482.

18. H. Q. Chen, J. C. Ren, *Talanta*, 2012, **99**, 404-408.

19. N. Shao, Y. Zhang, S. M. Cheung, R. H. Yang, W. H. Chan, T. Mo, K. A. Li, F. Liu, *Anal. Chem.*, 2005, **77**, 7294-7303.

20. K. C. Grabar, R. G. Freeman, M. B. Hommer, M. J. Natan, *Analytical Chemistry*, 1995, **67**, 735-743.

21. Z. P. Wang, J. Li, B. Liu, J. Q. Hu, X. Yao, J. H. Li, *J. Phys. Chem. B*, 2005, **109**, 23304-23311.

22. W. W. Yu, L. H. Qu, W. Z. Guo, X. G. Peng, *Chem. Mater.*, 2003, **15**, 2854-2860.

23. Chinese National Standards GB/T5009.199.2003, Standards Press of China,

445 Beijing, 2003.

446 24. G. Wu, H. Yu, X. Bao, H. Chen, Q. Ye, *Chin. J. Chromatogr*., 2007, **25**, 288-289.

447 (in Chinese).

448 25. H. Zhang, Z. Zhou, B. Yang, *J. Phys. Chem. B*, 2003, **107**, 8-13.